Journal of the Optical Society of Korea, Vol. 10, No. 1, March 2006, pp. 1-10

Analysis of Optical Properties with Photopolymers for Holographic Application

Nam Kim* and Eun Seop Hwang

Dept. of Computer & Communication Eng., Chungbuk Nat'l Univ., KOREA

Chang Won Shin

Prism Technology Inc., KOREA

(Received February 16, 2006 : revised March 13, 2006)

Optical transparency and high diffraction efficiency are two essential factors for high performance of the photopolymer. Optical transparency mainly depends on the miscibility between polymer binder and photopolymerized polymer, while diffraction efficiency depends on the refractive index modulation between polymer binder and photopolymerized polymer. For most of organic materials, the large refractive index difference between two polymers accompanies large structural difference that leads to the poor miscibility and thus poor optical quality via light scattering. Therefore, it is difficult to design a high-performance photopolymer satisfying both requirements. In this work, first, we prepared a new phase-stable photopolymer (PMMA) with large refractive index modulation and investigated the optical properties. Our photopolymer is based on modified poly (methyl methacrylate) as a polymer binder, acryl amide as a photopolymerizable monomer, triethanolamine as initiator, and yellow eosin as a photosensitizer at 532 nm. Diffraction efficiency over 85% and optical transmittance over 90% were obtained for the photopolymer. Second, Organic-inorganic nanocomposite films were prepared by dispersing an aromatic methacrylic monomer and a photo- initiator in organic-inorganic hybrid sol-gel matrices. The film properties could be controlled by optimizing the content of an organically modified silica precursor (TSPEG) in the sol-gel matrices. The photopolymer film modified with the organic chain (TSPEG) showed high diffraction efficiency ($\rangle$ 90%) under an optimized condition. High diffraction efficiency could be ascribed to the fast diffusion and efficient polymerization of monomers under interference light to generate refractive index modulation. The TSPEG modified photopolymer film could be successfully used for holographic memory.

OCIS codes : 090.2900, 090.7330, 090.2890

I. INTRODUCTION

Photopolymers have been exploited in a variety of applications requiring versatile holographic storage media, such as heads-up displays [1], data storage [2], holographic optical elements [3,4], and waveguides [5]. Photopolymer is one of the most attractive media for optical data storage and security applications due to their relatively large refractive index modulation, high sensitivity, high dynamic range, and low cost [6,7]. Also, photopolymers are worthy of consideration as a volume holographic materials because of several attractive advantages, which include a self developing capability, dry processing, good stability, thick emulsion, high sensitivity, large diffraction efficiency, high resolution, and nonvolatile storage. However, lack of the ideal holographic recording materials prevents commercial application of holographic storage system. Recently, advances in the chemistry and in the processing of photopolymers have enabled the production of photopolymer with significantly lower shrinkage and greater thickness [8,9]. So it's important that we make the optical system for applying the holographic application with photopolymers.

In this work, we will present the materials (PMAA, TSPEG). First, we report the optical properties of PMAA which shows high phase stability and large refractive index modulation. Second, we report the optical storage system with TSPEG, the organically modified silica film having organic side chains that can facilitate monomer diffusion for the holographic application.

II. PREPARATION OF PHOTOPOLYMER FILMS AND OPTICAL SYSTEM

2.1 Preparation of photopolymers

2.1.1 Preparation of PMMA

We introduce methacrylic acid (MAA) unit into PMMA by copolymerization in order to enhance the optical quality of photopolymer based on acryl amide without sacrificing the large refractive index modulation. The molecular structures of the polymer matrix and photosensitive components, in other words, photopolymerizable monomer, initiator, and photosensitizer, are shown in figure 1. Triethanolamine (TEA) was used as initiator and yellow eosin (YE) was used as photosensitizer sensitive at 532 nm. The P (MMA-co-MAA) copolymers were prepared by solution copolymerization of methyl methacrylate (MMA) and methacrylic acid (MAA) using AIBN as an initiator. To the reactor fitted with a mechanical stirrer, condenser, and nitrogen inlet and outlet, the mixed monomers and solvent (tetrahydrofuran, THF) were added, and then the mixture was heated to 70°C. After reaching 70°C, AIBN was injected and stirred for 24 hours under nitrogen atmosphere. After the polymerization was completed, the product solution was precipitated in diethyl ether, filtered, washed two times in methanol, and dried under vacuum for 12 hours. The acid content was calculated by the titration with 0.1 N sodium hydroxide/methanol solution. For the preparation of photopolymer, the mixture of the polymer matrix, acryl amide (AA), triethanolamine (TEA), and yellow eosin (YE) was dissolved in the weight ratio 60:20:20:0.06 in tetrahydrofuran (THF). The homogeneous solution was cast onto a glass substrate and then dried for 12 hours at ambient temperature in the dark. Thickness of the photopolymers was in the range of 70 ~110 μm. The microstructure of recorded gratings was investigated by scanning electron microscope (SEM).

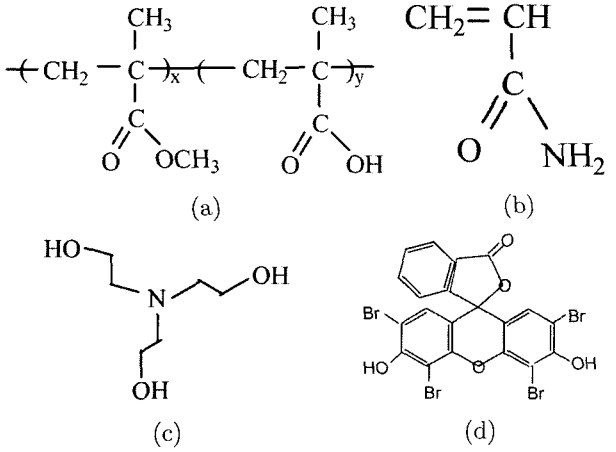

FIG. 1. (a) P (MMA-co-MAA) binder (b) Acryl amide (c) Triethanolamine (d) Yellow eosin.

For the SEM observation, polymer matrix phase was extracted out by dipping the photopolymer in THF for 12 hours after recording.

2.1.2 Preparation of TSPEG

An aromatic methacrylate monomer, 4,4'-sulfonylbis (phenyleneoxycarbonyloxy ethylmethacrylate) was synthesized from the bis (4-hydroxyphenyl) sulfone and ethylene glycol monomethacryl chloroformate as reported previously [10]. A sol-gel precursor (TSPEG) was synthesized from poly (ethylene glycol) methyl ether (PEGME) and 3-(triethoxysilyl)propyl isocyanate using dibutyltin dilaurate as a catalyst [11]. Chemicals and solvents were purchased from either Aldrich or TCI and purified according to the literature [12]. The organic-inorganic hybrid type solution was prepared by the sol-gel process using an organically modified precursor (TSPEG, [11]), 3-glycidoxyproplytrimethoxysilane (KH560), methyl trimethoxysilane (MTMS), and tetraethoxysilane (TEOS).

Photosensitive mixtures consisted of a monomer, a binder and a photoinitiator. Aromatic methacrylic and/or acrylic monomers (40 wt% total of the binder) was added to the sol-gel mixture (binder) in a brown bottle. Titanocene photoinitiator (Irgacure784, 2 wt% of the monomer) and tert-butylhydroperoxide (TBHP, 1/5 of the photoinitiator weight) were then added to the above mixture. The mixture was stirred with a magnetic stirrer and filtered using membranes of 0.45 μm pore size attached to a Teflon syringe. The solution was coated on glass plates, and thermally cured for 3~7 days at 60 -120°C

2.2 Mechanism of grating formation

The photopolymer material typically consists of polymeric binders, monomers, and plasticizers, along with initiating systems including photo-initiators, chain transfer agents, and sensitizing dyes. The binder acts as the support matrix containing the other film components. The monomers serve as refractive index "carrier". The choice of monomer and binder affects the physical properties of the film and the magnitude of index modulation (Δn) recorded in the film. The sensitizing dyes absorb light and interact with the photo-initiators to begin polymerization of monomers. The proper choice of components allows tailoring of material and holographic properties to specific applications or end uses. During holographic recording, the film is developing within an interference pattern formed by the intersection of two laser beams. The interference pattern consists of a sinusoidal variation of bright and dark fringes due to constructive and destructive interferences. In the process of making the bright fringes, the first sensitizing dye absorbs light. And second, it interacts with the initiators, and third, it creates free radicals, and then fourth, polymerization of the monomers occurs.

As monomer is converted to polymer in these regions, fresh monomer diffuses in from neighboring dark regions, thus setting up concentration and density gradients that result in refractive index modulation. During the exposure and polymerization processes, the initial high viscous composition gels and hardens, diffusion is suppressed, and further increase in the index modulation of the recorded hologram is fixed. At this point, we can make an easily viewable hologram through the film. The holographic image consists of polymer-rich regions that monomer diffused into and binder-rich regions that it diffused away from, with some residual unreacted monomer distributed throughout, as shown in Figure 3.

2.3 Effect of TSPEG on the monomer diffusion during the holographic recording

The holographic recording is based on the polymerization of the monomer under interfered light. The photopolymer film consists of sol-gel processed TSPEG modified silica network, aromatic monomers, and a photo-initiator. The silica network acts as the support matrix as well as a host for the monomers. Having flexible organic polyethylene glycol (PEG) group, TSPEG can have stronger interaction with organic monomers to result homogeneous film without phase separation between the media (inorganic silica network) and monomers (organic). In addition the resultant TSPEG modified silica network have more free volume to facilitate monomer diffusion.

The monomers serve as refractive index "carrier" since they are active under the interfered light. The choice of monomer and binder affects the physical properties of the film and the magnitude of index modulation (Δn) recorded in the film.

During holographic recording, the film is placed within an interference pattern formed by the intersection of two laser beams. The interference pattern consists of a sinusoidal variation of bright and dark fringes due to constructive and destructive interference. In the bright fringes, the initiators create free radicals, and polymerization of the monomers occurs. As monomer is converted to polymer in these regions, fresh monomer diffuses in from neighboring dark regions, thus setting up concentration and density gradients that result in refractive index modulation. During the exposure and polymerization processes, the initial highly viscous composition gels harden, then diffusion is suppressed, and further increase in the index modulation of the recorded hologram is established. The holographic recording consists of polymer-rich regions that monomer diffused into and binder-rich regions that it diffused away from, with some residual un-reacted monomer distributed throughout, as pictorially drawn in Figure 4.

Figure 5 shows diffraction efficiency determined by interfering two collimated plane wave beams of 532 nm using an optical set-up reported before [13]. The diffraction efficiency (DE) was increased sharply within 10 sec and reached a maximum of 98% with an exposure power of 5 mW. On the other hand, photopolymer film prepared without TSPEG showed low DE (Figure 5 (a)). High diffraction efficiency could be ascribed to the fast diffusion and efficient polymerization of monomers under interference light to generate large refractive index modulation. Thus, the silica matrix modified with the organic chain (TSPEG) may facilitate efficient monomer transport since the organic PEG has low glass transition temperature (Tg) and thus afford large free volume in the silica network. If so, the channel for the monomer diffusion should be wider for photopolymer films prepared with TSPEG compared to that without TSPEG (Figure 5). Therefore monomer diffusion could be controlled by the TSPEG content in the binder solution.

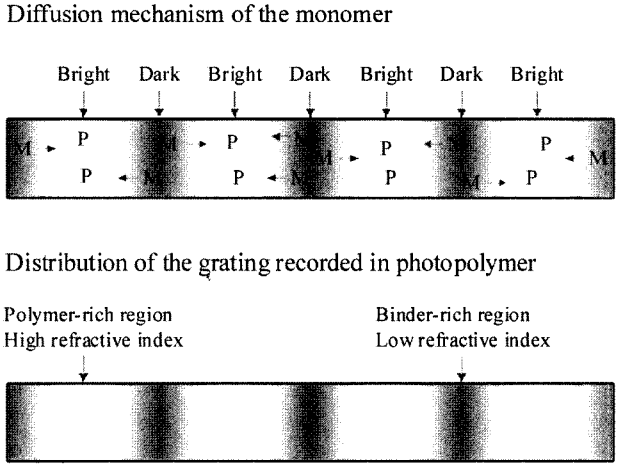

FIG. 2. Process of the index modulation in photopolymer.

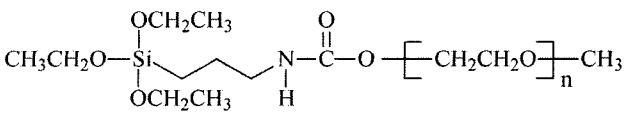

FIG. 3. Chemical structure of TSPEG.

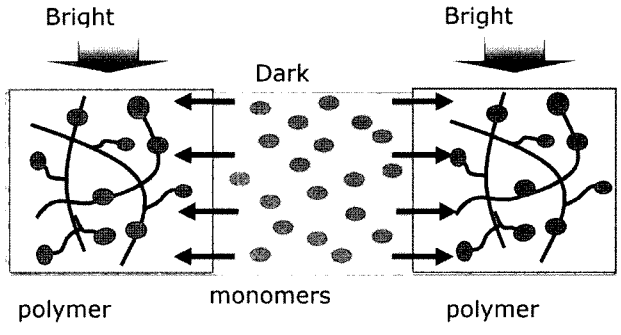

FIG. 4. Scheme for monomer diffusion by interference fringes (b) Monomer diffusion assisted by TSPEG.

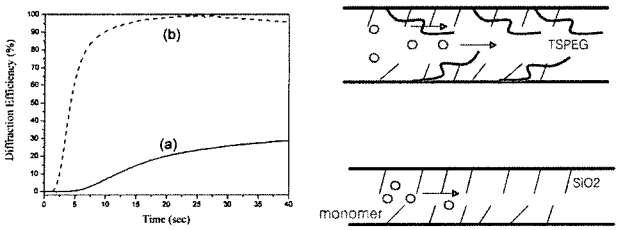

FIG. 5. DE (%) as a function of exposure time for a 200 μm thick film prepared (a) without and (b) with TSPEG (0.25 mol%).

2.4 Diffraction efficiency

In 1960 H. Kogelnik introduced the coupled-wave theory [14], which can predict the maximum possible efficiencies of the various hologram types, and the angular and wavelength dependence at high diffraction efficiencies. The formula of the diffraction efficiency with transmission-type hologram is given by

$$\eta = \sin^2\left[\frac{\pi \Delta n d}{\lambda(\cos\theta_R \cos\theta_S)^{1/2}}(r\cdot s)\right] \quad (1)$$

where, Δn is the refractive index modulation, d is the grating thickness, λ is the operating wavelength, θ_R is the reconstruction angle between the reconstruction beam R and z axis, θ_S is the diffraction angle made by the diffracted beam S and z axis, and are the unit vectors in the direction of the reconstruction and diffracted-beam polarization vectors. If the reconstruction beam is s-polarized, the product of $r \cdot s$ is equal to unity. When a p-polarized reconstruction beam is used, $r \cdot s = \cos(\theta_S - \theta_R)$. Consequently, the efficiency in Eq. (1) can be rewritten for the two orthogonal modes of polarization as follows

$$\eta_{s,p} = \sin^2 \nu_{s,p} \quad (2)$$

where, the grating strength ν_s, ν_p are given by

$$\nu_s = \frac{\pi \Delta n d}{\lambda(\cos\theta_R \cos\theta_s)^{1/2}} \quad , \quad (3)$$

$$\nu_p = \frac{\pi \Delta n d}{\lambda(\cos\theta_R \cos\theta_s)^{1/2}} \cos(\theta_S - \theta_R) \quad . \quad (4)$$

2.5 Optical system set-up for holographic application

2.5.1 Optical system set-up for holographic recording (material : PMAA)

Figure 6 shows the experimental setup to measure optical properties of the photopolymer for holographic applications such as holographic storage, optical filter [14], polarization elements, optical switch, and so on. A continuous wave (CW) Nd-YAG laser (λ = 532 nm) was used for the two recording beams. The system

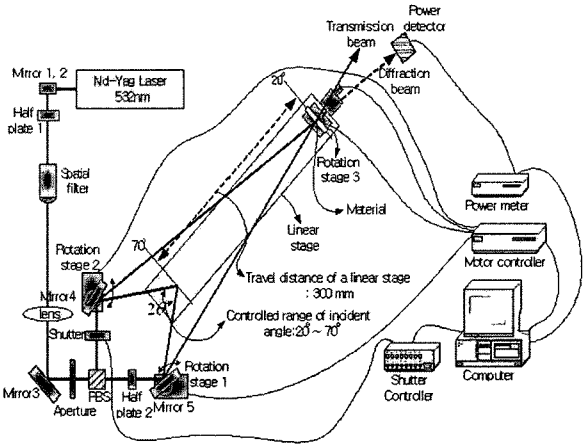

FIG. 6. Optical setup for holographic recording.

consisted of a linear stage with the travel distance of 300 mm and rotation stages to control an incident angle. In this system, the available range of the incident angle is between 20°~70°. To detect a diffracted beam, an electrical shutter was used in the object beam arm. When the shutter blocks the object beam, only the reference beam strikes the sample. The reference beam is deflected into the direction of the object beam as the hologram grows and can be detected with a photo detector, which is connected to a computer. In this method, the Bragg relation was automatically satisfied and changes in thickness did not influence measurements of diffraction efficiencies [15]. The blocking time of the electric shutter to measure the diffraction efficiency of photopolymer films was programmed with 0.5 sec and the exposure time of the beams for holographic recording was 20 sec. A power ratio of the two beams could be varied by the adjustable PBS, which consists of a rotation half-wave plate, followed by a polarizing beam-splitter cube and a fixed half wave plate, as shown in Figure 6. However the power ratio between the signal and reference beam was equal to 1:1 for achieving the maximum modulation ratio. The two beams were overlapped on the holographic medium and the interference pattern by the two beams was recorded in the film.

2.5.2 Optical system set-up for holographic data storage with SLM(material :TSPEG)

Another experimental setup has been used for image monitoring of the holographic data storage (Figure 7). The laser source for these experiments was coherent frequency-doubled Nd:YAG laser at 532 nm. Here we used the coherent frequency laser for acquiring the information about different phases. The reference beam and signal beam were incident at $\pm 30^\circ$ with respect to the recording materials surface normal and the optical powers of the signal and the reference beams were 0.66 mW /cm^2 and 2.1 mW/cm^2, respectively. Here, we got diffe-

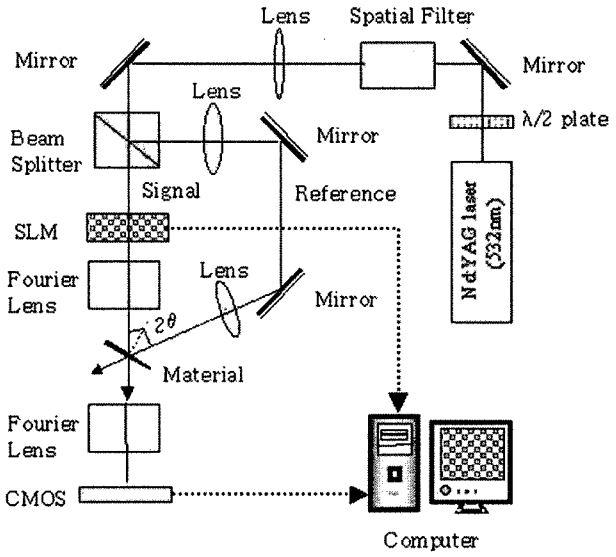

FIG. 7. Experimental setup for holographic data storage with SLM

rent intensities between signal beam and reference beam for reducing signal beam intensity through the SLM. In this holographic data storage set up, data were converted to an optical signal using a spatial light modulator (SLM). Readout of stored data page involved illuminating the films, the reference beam, and imaging the diffracted optical signal onto a CCD (MVOS CMOS camera) array, which converts the optical signal back into an electronic signal. For this purpose, motorized and computer controlled linear stage for spatial multiplexing and electronic-shutter were used. The SLM was based on 640×480 pixel liquid crystal (EPSON VGA LCTV), and pixel matching of SLM-CCD was 1: 3 over sampling.

3. RESULTS AND DISCUSSIONS

3.1 Results of the experiment for holographic recording

3.1.1 Diffraction efficiency of the materials versus incident angle and exposure energy

Figure 8 shows the temporal traces of diffraction efficiency for the photopolymer with different incident angles. The intensities of the recording beams were set at 4.3 mW/cm^2. We measured the diffraction efficiency of materials as a function of a full incident angle. Several samples of material were recorded symmetrically at the range of the incident angles from 20° to 70°. Similar behaviors of grating buildup were obtained for different incident angles. Diffraction efficiencies over 90% were obtained except for the grating recorded at incident angle of 70°. And, when exposure was allowed to continue, the efficiencies of gratings were saturated. As a result of the experiment, figure 8 shows the diffract-

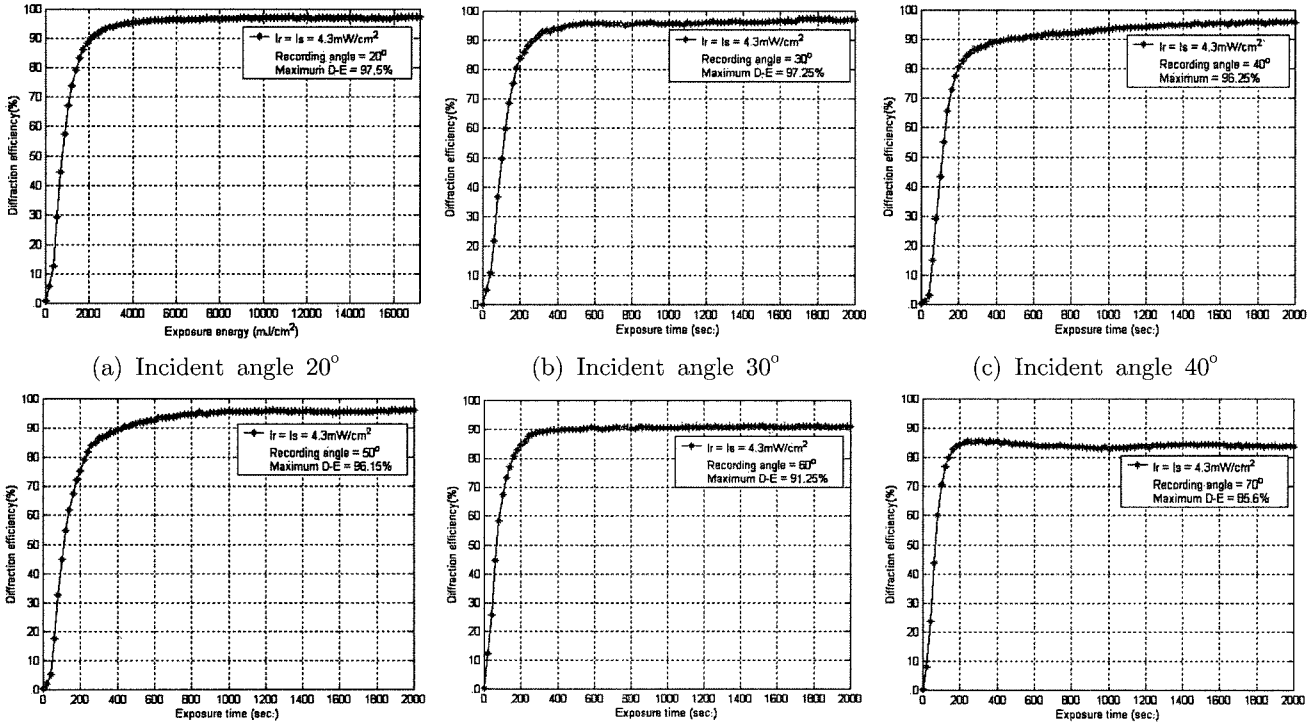

(a) Incident angle 20° (b) Incident angle 30° (c) Incident angle 40°

(d) Incident angle 50° (e) Incident angle 60° (f) Incident angle 70°

FIG. 8. The diffraction efficiency of the photopolymers.

ion efficiencies of samples as a function of the incident angle on the materials. Figure 8 (a) describes the diffraction efficiency versus the recording time and figure 8 (b) describes the diffraction of the hologram versus exposure energy. The diffraction efficiencies of materials at the angles from 20° to 50° were almost equal. However, the highest diffraction efficiency was observed at the angle of 20°. And Energetic sensitivity of the photopolymer was measured as 4 J/cm^2 at incident angle of 20°.

3.1.2 Angular selectivity of photopolymer

Multiple holograms for digital holographic memory are overlapped at each location by the used of hologram-multiplexing methods such as angle, wavelength, phase-code, fractal, peristrophic, and shift multiplexing [16]. Angular selectivity is one of the important parameters for angular multiplexing page oriented holographic memories (POHMs) because it determines the total number of sub-holograms with a small cross-talk. We define the angular selectivity is first null point in Figure 8. In this experiment, we measured the angular selectivity of the materials for the multiplexing. The dependence of diffraction efficiency on the angular detuning $\Delta\theta$ is shown in Figure 8.

$$\Delta\theta = (\Delta\theta)_B = \frac{\lambda}{2d\ \sin\theta} \quad , \tag{5}$$

Where, λ is the wavelength of beam (λ= 532 nm), d is the thickness of material, θ is the half of the external angle between two recording beams. The diffraction efficiency is maximum when $\Delta\theta = 0$; this condition is called Bragg matching. The average refractive index of 1.56 was used for the estimation. When Eq. 5 reaches its first null, the hologram does not diffract the incident light at all. The quantity $(\Delta\theta)_B$ is called the angular selectivity [17]. Figure 10 (a) shows the simulation results of the diffraction properties and the angular selectivity in dependence on the incident angle. Also, Figure 10 (b) shows the results for the optical properties in dependence on film thickness.

At the angular selectivity curve, measured main lobe curves of the curves are in good agreement with theoretical value. However, measured side lobe curves are slightly different from the theoretical value because the surface of the photopolymer is not completely flat. The thickness of the photopolymers was measured using a vernier callipers with resolution of 10 μm to compare the measured and theoretical values of the angular selectivity. Table 1 shows the relation between the theoretical and measured angular selectivity of the materials.

As a result of experiment for the angular selectivity, a curve of the theoretical value and the experimentally measured value of the selectivity were in good agreement as shown in Figure 9. This result confirms the fact that the change in the angular selectivity is caused

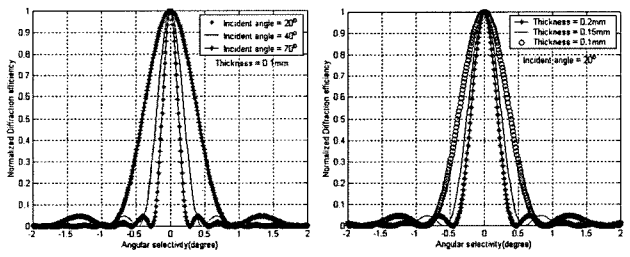

(a) (b)

FIG. 9. Angular selectivity of holographic grating (a) Constant thickness (b) Constant incident angle.

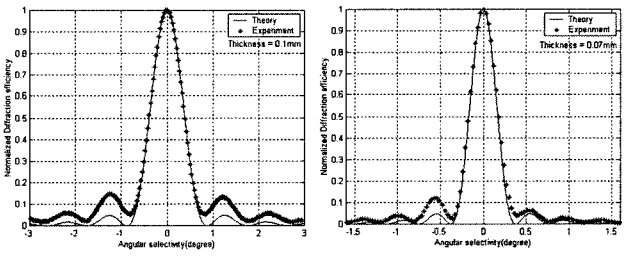

(a) (b)

FIG. 10. angular selectivity of holographic grating at (a) incident angle of 20° and (b) incident angle of 70°.

TABLE 1. Angular selectivity of samples with different incident angles and thickness of the photopolymer films.

External incident angle (Half angle)	Thickness (mm)	Angular selectivity (Degree) (Theory)	Angular selectivity (Degree) (Experiment)
20 (10)	0.1	0.877	0.87
30 (15)	0.09	0.654	0.63
40 (20)	0.08	0.557	0.54
50 (25)	0.09	0.400	0.39
60 (30)	0.08	0.381	0.39
70 (35)	0.07	0.379	0.36

by the thickness change of photopolymer.

3.1.3 Spatial frequency of recorded the grating

After holographic recording, we observed the period of the recorded gratings in the photopolymer using a scanning electron microscope (SEM). We compared the measured period of the grating using the microscope with the theoretical value of the grating period. The results are summarized in Table 2.

The period of the grating was inversely proportional to incident angle of recording beams by Eq. 6 and Figure 11 shows a typical microstructure of grating recorded at incident angle of 35°. By comparing the grating period shown in Figure 11. and the theoretical grating period, the observed grating period is in good agreement with the theoretical value.

$$\Lambda = \frac{\lambda}{2n \sin\theta} \tag{6}$$

where, represents the period of holographic grating in material, λ represents the wavelength of the recording beam, n = 1.48 represents the average index of photopolymer and θ represents the internal incident angle (half angle) of recording beams. At incident angle of 35°, theoretical value of the grating period was about 0.88 μm and the measured grating period by the SEM was nearly 0.9 μm, which indicates the good agreement between theoretical grating period and observed period.

3.2 Results of the experiment for holographic data storage with SLM

3.2.1 Diffraction efficiency of the photopolymer vs. exposure time and energy

Figure 12. shows the diffraction efficiency dependent on the exposure time (and exposure energy) for the optimized photopolymer film containing TSPEG (0.25 mol%), using the set-up in Figure 7. The recording angle, which can be adjusted by the rotation stage, was fixed at 35°. The intensities of two recording beams were set at 2.1 mW/cm^2. The diffraction efficiency reached 96% with an exposure energy of about 210 mJ/cm^2. When exposure was allowed to continue, the efficiency began to drop slightly and then kept constant.

TABLE 2. The grating period of samples with different incident angles.

External incident angle (Half angle)	Grating period (m) (Theory)	Grating period (m) (Experiment)
35 (17. 5)	0.8846	0.9

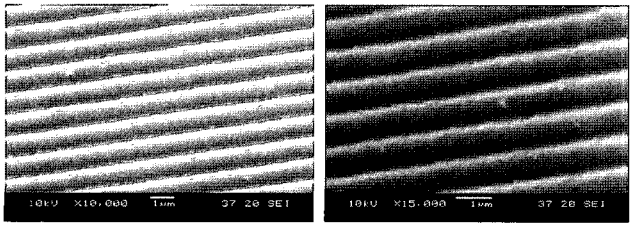

FIG. 11. The microstructure of gratings recorded at incident angle of 35°.

3.2.2 Diffraction efficiency of photopolymer films with different incident beam angles

We measured the diffraction efficiency of materials as a function of a full incident angle of beams. The first several samples of material were recorded symmetrically at the range of the incident angles from 20° to 70° using the optical system (Figure 6) for acquiring the high diffraction efficiency in the hologram storage system. The intensities of the recording beams were set at 2.1 mW/cm^2. Figure 13. shows the maximum diffraction efficiencies of samples as a function of the incident angle on the materials. The diffraction efficiencies of photopolymer films at the angles from 30°~40° were almost equal. However, the highest diffraction efficiency was observed at 35°. we applied that in the hologram storage system (Figure 7).

3.2.3 Angular selectivity of the photopolymer film (TSPEG)

Angular selectivity is one of the important parameters for angular multiplexing page oriented holographic mem-

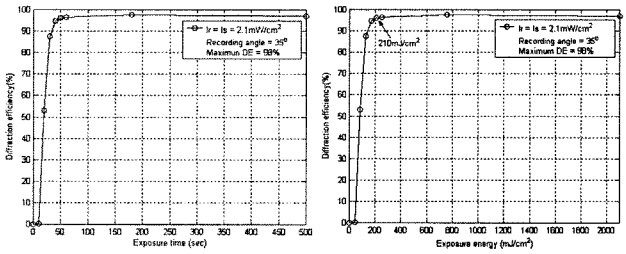

(a) (b)

FIG. 12. Diffraction efficiency of the hologram as (a) exposure time (b) exposure energy.

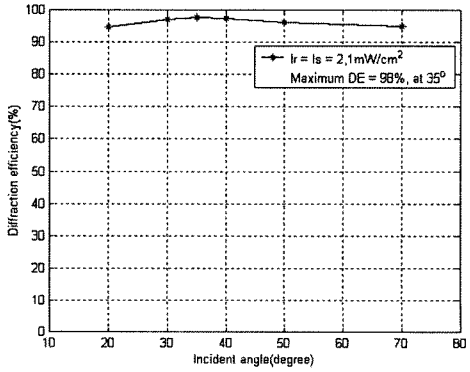

FIG. 13. Diffraction efficiency verse incident angle.

ories (POHMs) because it determines the total number of sub-holograms with a small cross-talk. At this experiment, we measured the angular selectivity of the materials for the multiplexing. The dependence of η (diffraction efficiency) on the angular detuning ($\Delta\theta$) is described by the Eq. 5 as shown in Figure 14.

Figure 14 (a) shows simulated plot of the diffraction efficiency (η) against the angular selectivity ($\Delta\theta$) at two different incident angles, indicating that the angular selectivity is highly dependent on the incident angles. Figure 14 (b) show simulated plot of η against $\Delta\theta$ using two photopolymers having different film thickness. When the film thickness is larger, $\Delta\theta$ is smaller, as one can expect from the Eq. 5

Figure 15. shows the experimental results of η vs $\Delta\theta$ for the photopolymers prepared with TSPEG (0.25 mol). The experimental curves for photopolymer films having different thickness were completely overlapped with the simulated plot, indicating that the holographic recording on the photopolymer film follows ideal behavior.

Since angular selectivity of the photopolymer films depends on their thickness, the thicknesses of the films were measured using a vernier callipers with resolution of 0.01 mm to analyze the measured and theoretical values of the angular selectivity. After the recording, we measured the thickness of the materials to calculate the theoretical value of the angular selectivity. Table. 3 shows the relation between the theoretical and experimentally determined angular selectivity of the materials, indicating that the experimental results correlate well to the theoretical value. This result confirmed that the change of the angular selectivity is caused by the change of the film thickness.

3.2.4 Reconstruction of a digital image and a real image

High capacity data storage demands near-perfect fidelity of the reconstructed image. The original image, therefore, must be recorded clearly and must be free of distortions or blurring. We recorded a digital image and a real object in the photopolymer films using the experimental setup in Figure 7. The laser source for digital image recording experiment was coherent frequency- doubled Nd:Yag laser at 532 nm. Reference beam and signal beam were incident at $\pm 30^{\circ}$ with respect to the recording material surface normal. Digital image was recorded onto a pixelated spatial light modulator with rectangular pixel aperture and reconstructed on the photopolymer film. Figure 16. (a) and (b) show the reconstructed data of a digital image (78×54 bits) and a reconstructed the real image (image of real object), respectively, stored in the photopolymer film.

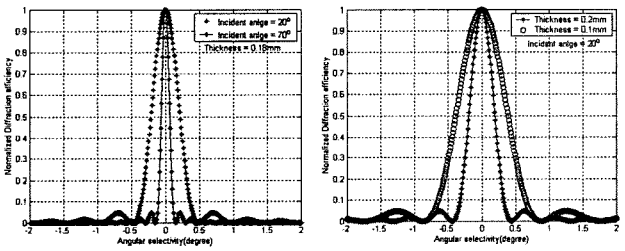

(a) (b)

FIG. 14. Angular selectivity of holographic grating (a) Constant thickness (b) Constant incident angle.

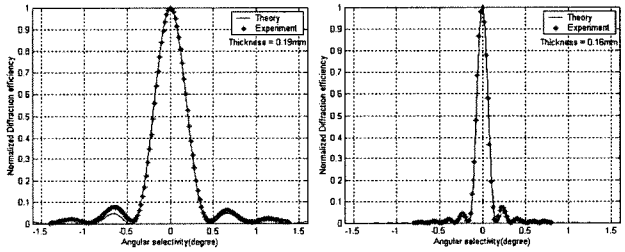

(a) (b)

FIG. 15. Angular selectivity of holographic grating at an incident angle of 20° (a) and of 70° (b).

TABLE 3. Angular selectivity of photopolymer films

Incident angle(half) (degree)	Thickness (mm)	Theory (degree) (Angular selectivity)	Experiment (degree) (Angular selectivity)
20 (10)	0.19	0.4619	0.46
30 (15)	0.2	0.2944	0.29
35 (17.5)	0.15	0.3378	0.34
40 (20)	0.18	0.2475	0.24
50 (25)	0.14	0.2575	0.25
70 (35)	0.16	0.166	0.16

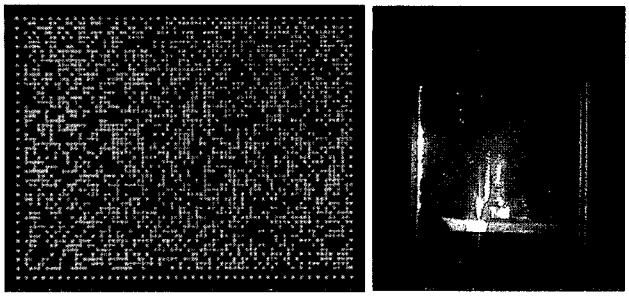

(a) (b)

FIG. 16. (a) Reconstructed data of a digital image (78×54 bits) and (b) a real image (image of real object) stored in the photopolymer film.

5. CONCLUSIONS

We investigated the optical properties of two different photopolymers (PMAA and TSPEG) for holographic application. First, in a material (PMAA) made in KAIST, The photopolymer shows very high diffraction efficiency over 90%. The maximum diffraction efficiency of the photopolymer were measured about 98% at incident angle of 20°~30°. Energetic sensitivity of the photopolymer is measured as 4 J/cm^2 at incident angle of 20°. The angular selectivity of the photopolymer was measured as a function of the incident angle from 20° to 70° and the measured and theoretical values of angular selectivity were in good agreement. After recoding, we compared the spatial frequency of the recoded grating by analyzing the microstructure of recorded grating and the measured value of grating period and the theoretical value were in good agreement.

Second, in a material (TSPEG) made in KRICT, we demonstrated that the organic-inorganic hybrid photopolymer film could be successfully used for holographic recording. Such photopolymer films were prepared using a mixture of aromatic methacrylic monomer, photoinitiator and an organically modified sol-gel mixture. High diffraction efficiency and fast response for the photopolymer prepared with TSPEG were ascribed to the effective monomer diffusion assisted by PEG group in the organically modified sol-gel mixture. The maximum diffraction efficiency of the film was 98% at incident angle of 35°. The diffraction efficiencies of the recorded photopolymers at different intensities in the range from 0.1 mW/cm^2 to 10 mW/cm^2 were from 96% to 98%. The photosensitivity of the photopolymer was about 210 mJ/cm^2 at the incident angle of 35°. The angular selectivity of the films as a function of incident angle was determined at the incident angle from 20° to 70°. The experimental and the theoretical value were in good agreement. A digital holographic image (78×54 bits) and a real object were recorded successfully in the photopolymer.

ACKNOWLEDGEMENT

This work was supported by the research grant of the Chungbuk National University in 2005

*Corresponding author : namkim@chungbuk.ac.kr

REFERENCE

[1] W. Chao and S. Chi, "Diffraction properties of windshield laminated photopolymer holograms," *J. Opt.*, vol. 29, pp. 95-103, 1998.

[2] A. Pu and D. Psaltis, "High-density recording in photopolymer based holographic three-dimensional disks," *Appl. Opt.*, vol. 35, pp. 2389-2398, 1996.

[3] W. Gambogi, K. Steijn, S. Mackara, T. Duzick, B. Hamzavy, and J. Kelly, "HOE imaging in Dupont holographic photopolymer," in *Diffractive and Holographic Optics Technology*, I. Cindrich and S. H. Lee, eds., Proc. SPIE., vol. 3294, pp. 207-214, 1998.

[4] J. E. Ludman, J. R. Riccobono, N. O. Reinhand, I. V. Semenova, Y. L. Korzinin, S. M. Shahriar, H. J. Caulfield, J. M. Fournier, and P. Hemmer, "Very thick holographic nonspatial filtering of laser beams," *Opt. Eng.*, vol. 36, pp. 1700-1705, 1997.

[5] T. J. Trout, J. J. Schmieg, W. J. Gambogi, and A. M. Weber, "Optical photopolymers: design and application," *Adv. Mat.*, vol. 10, pp. 1219-1224, 1998.

[6] J. T. Gallo and C. M. Verber, "Model for the effects of material shrinkage on volume holograms," *Appl. Opt.*, vol. 33, pp. 6797-6804, 1994.

[7] L. Dhar, M. G. Schnoes, T. L. Wysocki. H. Bair, M. Schilling, and C. Boyd, "Temperature induced changes in photopolymer volume holograms," *Appl. Phys. Lett.*, vol. 73, pp. 1337-1339, 1998.

[8] L. Dhar, K. Curtis, M. Tackitt, M. Schilling, S. Campbell, W. Wilson, A. Hill, C. Boyd, N. Levinos, and A. Harris, "Holographic storage of multiple high capacity digital data pages in thick photopolymer systems," *Opt. Lett.*, vol. 23, pp. 1710-1712, 1998.

[9] V. L. Colvin, R. G. Larson, A. L. Harris, and M. L. Schilling, "Quantitative model of volume hologram formation in photopolymers," *J. Appl. Phys.*, vol. 81, pp. 5913-5923, 1997.

[10] J. Park and E. Kim, "Preparation and holographic recording of an organic-inorganic hybrid type photopolymer film," *J. Kor. Soc. Imaging. Sci*, vol. 8 (2002), 22.

[11] H. J. Kim, Y. B. Han, W. N. Kim, and E. Kim, "Electrochromic Poly (aniline-N-butylsulfonate)s and Their Application to Electrochromic devices," *J. Jap. Soc. Colour Mater.*, vol. 72 (1999), 11.

[12] W. L. F. Armarego and D. D. Perrin, *Purification of Laboratory Chemicals* (Butterworth Heinemann Publications, Oxford (1996).

[13] E. Kim, J. Park, S. Y. Cho, J. H. Kim, and N. Kim, "Preparation and holographic recording of diarylethene doped photochromic films," *ETRI Journal*, vol. 25 (2003), 253.

[14] G. Barbastathis and D. Psaltis, "Volume holographic

multiplexing methods," *Holographic Data Storage*, pp. 21-62, 2000

[15] Ducdung Do, Junwon An, and Nam Kim "Gaussian Apodization Technique in Holographic Demultiplexer Based on Photopolymer," *J. Optical Society of Korea*, vol. 7, no. 4, pp. 269-274, 2003.

[16] A. Fimia, F. Mateos, A. Belendenz, R. Mallavia, F. Amat-Guerri, and R. Sastre, "New photopolymer with tri-functional monomer for holographic application," *Appl. Phys. B.*, vol. 63, pp. 151-153, 1996.

[17] H. Kogelnik, "Coupled wave theory for thick hologram gratings," *Bell Syst. Tech. J.*, vol. 48, pp. 2909-2947, 1969.